Chemistry of Metals and Alloys

Chem. Met. Alloys 16 (2023) 7-13
Ivan Franko National University of Lviv
http://publications.lnu.edu.ua/chemetal

Hydrogenation of Dy_2Ni_2In and Al- and Ga-substituted derivatives

Khrystyna MILIYANCHUK[1]*, Ladislav HAVELA[2], Silvie MAŠKOVÁ-ĆERNÁ[2], Roman GLADYSHEVSKII[1]

[1] *Department of Inorganic Chemistry, Ivan Franko National University of Lviv, Kyryla i Mefodiya St. 6, 79005 Lviv, Ukraine*
[2] *Department of Condensed Matter Physics, Charles University, Ke Karlovu 5, 121 16 Prague 2, Czech Republic*
* *Corresponding author. E-mail: khrystyna.miliyanchuk@lnu.edu.ua*

Received April 19, 2023; accepted June 29, 2023
https://doi.org/10.30970/cma16.0429

Hydrogenation properties of the compounds Dy_2Ni_2In (Mn_2AlB_2 structure type, Pearson symbol *oS*10, space group *Cmmm*) and $Dy_2Ni_2In_{0.8}X_{0.2}$ (*X* = Al, Ga) (Mo_2FeB_2 structure type, Pearson symbol *tP*10, space group *P*4/*mbm*) were studied at room temperature under hydrogen pressures below ambient. Hydrides of compositions $Dy_2Ni_2InH_{4.5}$, $Dy_2Ni_2In_{0.8}Al_{0.2}H_{4.2}$, and $Dy_2Ni_2In_{0.8}Ga_{0.2}H_{3.7}$ were synthesized. In all cases, the arrangement of the metal atoms was preserved after hydrogenation. Hydrogenation resulted in anisotropic lattice modification, which prevailed in one direction (along the *a*-axis) for the Mn_2AlB_2-type compound and in a plane (*ab*-plane) for the Mo_2FeB_2-type compounds. The role of individual structure fragments in the hydrogenation process is discussed.

Intermetallic / Hydride / X-ray diffraction / Crystal structure

1. Introduction

The structure types Mn_2AlB_2 (Pearson symbol *oS*10, space group *Cmmm*, atomic coordinates Mn in 4*j* (0, *y*, ½), B in 4*i* (0, *y*, 0), Al in 2*a* (0, 0, 0) [1]) and Mo_2FeB_2 (Pearson symbol *tP*10, space group *P*4/*mbm*, atomic coordinates Mo in 4*h* (*x*, *x* + ½, ½), B in 4*g* (*x*, *x* + ½, 0), Fe in 2*a* (0, 0, 0) [2]) belong to a structure series with the general formula $R_{m+n}T_{2m}M_n$, based on the binary types AlB_2 (face-sharing filled trigonal prisms $\underline{T}R_6$) and CsCl (filled deformed cubes $\underline{M}R_8$), where *R*, a rare-earth element, represents the largest atoms, *T*, a *d*-element, the smallest atoms, and *M*, a main-group element, the atoms of intermediate size [3]. Mn_2AlB_2 is an inhomogeneous 1D intergrowth structure, while Mo_2FeB_2 is an inhomogeneous 2D intergrowth structure (Fig. 1). Both structure types are formed in *R*–Ni–In systems [4]. The orthorhombic structure type Mn_2AlB_2 is adopted by the R_2Ni_2In compounds with *R* = Y, Gd–Lu in as-cast state and after annealing, while for Sm_2Ni_2In it corresponds to the low-temperature modification (after annealing at 600°C or lower temperatures). For other conditions and/or rare-earth metals, the tetragonal type Mo_2FeB_2 is observed. Moreover, vacancies in the position of Ni lead to the formation of off-stoichiometric compounds $R_2Ni_{2-x}In$ ($x \approx 0.22$) with Mo_2FeB_2-type structure for the full rare-earth metal series, both in as-cast state and after annealing.

Compounds crystallizing with the tetragonal Mo_2FeB_2-type structure have been widely studied for hydrogenation. It was found that their hydrogenation properties strongly depend on the chemical composition [5,6]. Within the series R_2Ni_2In, hydrogenation properties have been reported for the compounds where *R* = La, Ce, Pr, Nd [7,8]. They absorb up to 4.5-5 hydrogen atoms per formula unit (H at./f.u.) at hydrogen pressures below ambient, and 7 H at./f.u. at a hydrogen pressure of 7 bar. Hydrogenation is accompanied by a decrease in symmetry to orthorhombic (space group *Pbam*). The hydrogen atoms occupy four independent positions: one inside an octahedron [R_4NiIn], one inside a trigonal bipyramid [R_3Ni_2], and two inside tetrahedra [R_2Ni_2] and [R_2In_2].

There are no data available on hydrogenation properties of compounds with the closely related structure type Mn_2AlB_2. The aim of the present work was to study the hydrogenation properties of the compound Dy_2Ni_2In, crystallizing with the orthorhombic Mn_2AlB_2 structure type, and to compare them with those of related compounds with the tetragonal Mo_2FeB_2 structure type.

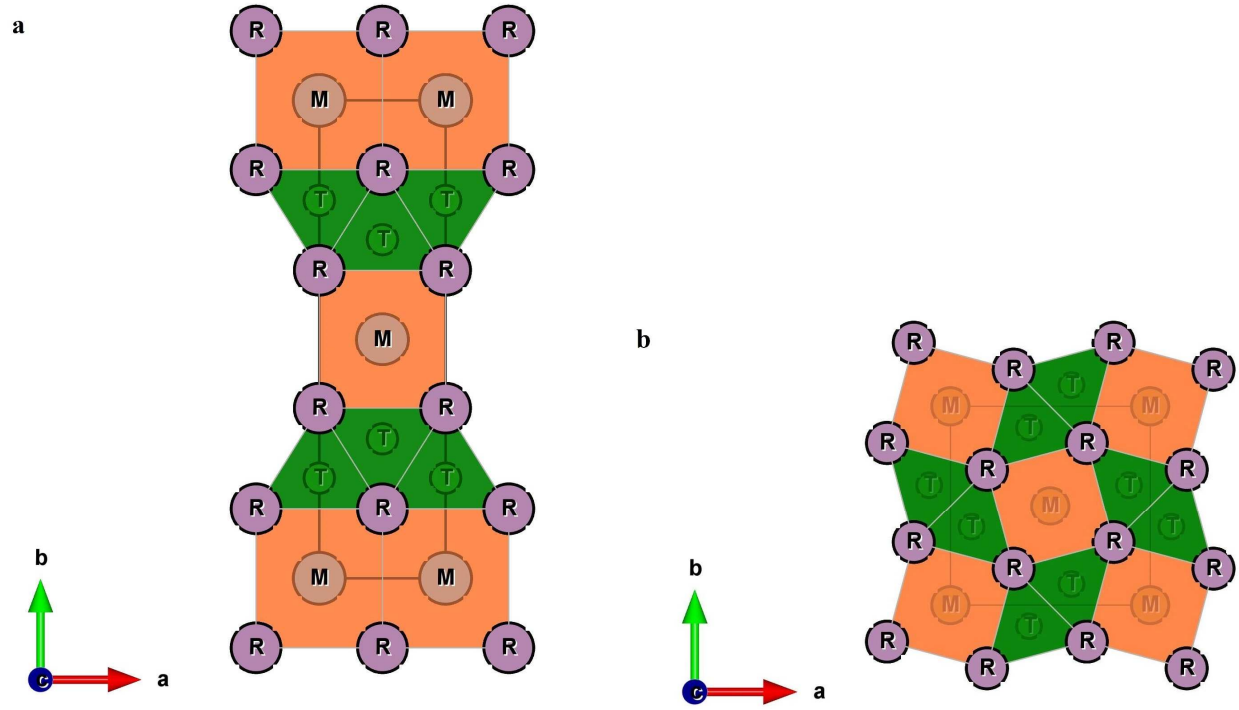

Fig. 1 Representation of the Mn_2AlB_2 (a) and Mo_2FeB_2 (b) structure types belonging to the structure series $R_{m+n}T_{2m}M_n$, based on the binary types AlB_2 (*m*, green) and CsCl (*n*, orange).

2. Experimental details

The intermetallic compounds were synthesized by arc-melting elemental metals of at least 99.9 % purity under argon atmosphere. Selected samples were later annealed in evacuated quartz ampoules at 600°C for two months. The composition was checked by estimating the weight losses after melting. The samples were further examined by scanning electron microscopy, using a Vega 3 LMU (Tescan) microscope, equipped with an X-ray energy-dispersive analyzer Flash (Bruker) for quantitative probe microanalysis by energy-dispersive spectroscopy (EDS).

Hydrogenation was performed exposing the alloy, crushed before into submillimeter particles and activated by heating up to 250°C for 2 h in oil-free vacuum ($\approx 5\cdot10^{-6}$ mbar), to H_2 gas (p = 700-870 mbar). The hydrogen absorption was estimated by measuring the pressure drop in a closed system. The thermal stability of the hydride was subsequently checked by heating up to 700°C in a closed system.

The crystal structures were studied at room temperature by X-ray powder diffraction, on a STOE Stadi P diffractometer (Cu $K\alpha_1$ radiation) or a Bruker D8 Advance diffractometer (Cu $K\alpha$ radiation). The crystal structure refinements were based on the Rietveld algorithm, using the program package FullProf Suite [9]. Differential scanning calorimetry (DSC) curves were obtained using a Linseis STA PT 1600 system in dynamic argon atmosphere (5 L/h) with heating and cooling rates of 10 K/min in the temperature range 20-1100°C.

3. Results

3.1 Hydrogenation of Dy_2Ni_2In

Hydrogenation of the Dy_2Ni_2In sample (Mn_2AlB_2 structure type), annealed at 600°C, was performed at room temperature under hydrogen at a pressure of 700 mbar. The reaction started after an incubation time of ~2 h and went on for another 3 h. The total pressure drop corresponded to the hydride composition $Dy_2Ni_2InH_{4.5}$. The results of the X-ray diffraction analysis showed that after hydrogenation the sample contained a main phase with the Mn_2AlB_2 structure type, and a minor amount of Dy_2O_3, which could have formed after exposing the sample to air. The peak broadening in the X-ray powder pattern indicates a non-negligible reduction of the size of the crystalline grains, or even some amorphization of the sample (Fig. 2a,b).

The type of crystal structure of the metallic matrix is preserved after hydrogenation. However, hydrogenation leads to strongly anisotropic lattice modification (Table 1). The prevailing direction of lattice expansion is the *a*-axis, meaning simultaneous stretching of the intergrown slabs with CsCl- and AlB_2-type structures along a single direction. At the same time, in the direction of the stacking of the slabs, *i.e.* along the *b*-axis, even a certain lattice contraction is observed.

The decomposition curve for the hydride $Dy_2Ni_2InH_{4.5}$ (Fig. 3) revealed the start of the desorption process already at 130°C. A second step of hydrogen release developed at 270°C. However, temperature increase above 480°C resulted in a pressure drop in the system, meaning reversed hydrogen sorption, which can be explained by a decomposition of the intermetallic with the formation of a simpler hydride. Further heating up to 700°C resulted in more hydrogen gas released, but upon cooling some amount of the hydrogen was reabsorbed. The reflections of the X-ray powder pattern collected for the sample after desorption denied the presence of the phase Dy_2Ni_2In or its hydride. Instead, the sample contained the phases DyNiIn (50.3 %), $DyNi_2$ (25.3 %), DyH_2 (11.2 %), and Dy_2O_3 (13.2 %) (Fig. 2c), meaning that the hydride $Dy_2Ni_2InH_{4.5}$ decomposes upon heating with the formation of the binary hydride DyH_2, which exists up to 840°C [10].

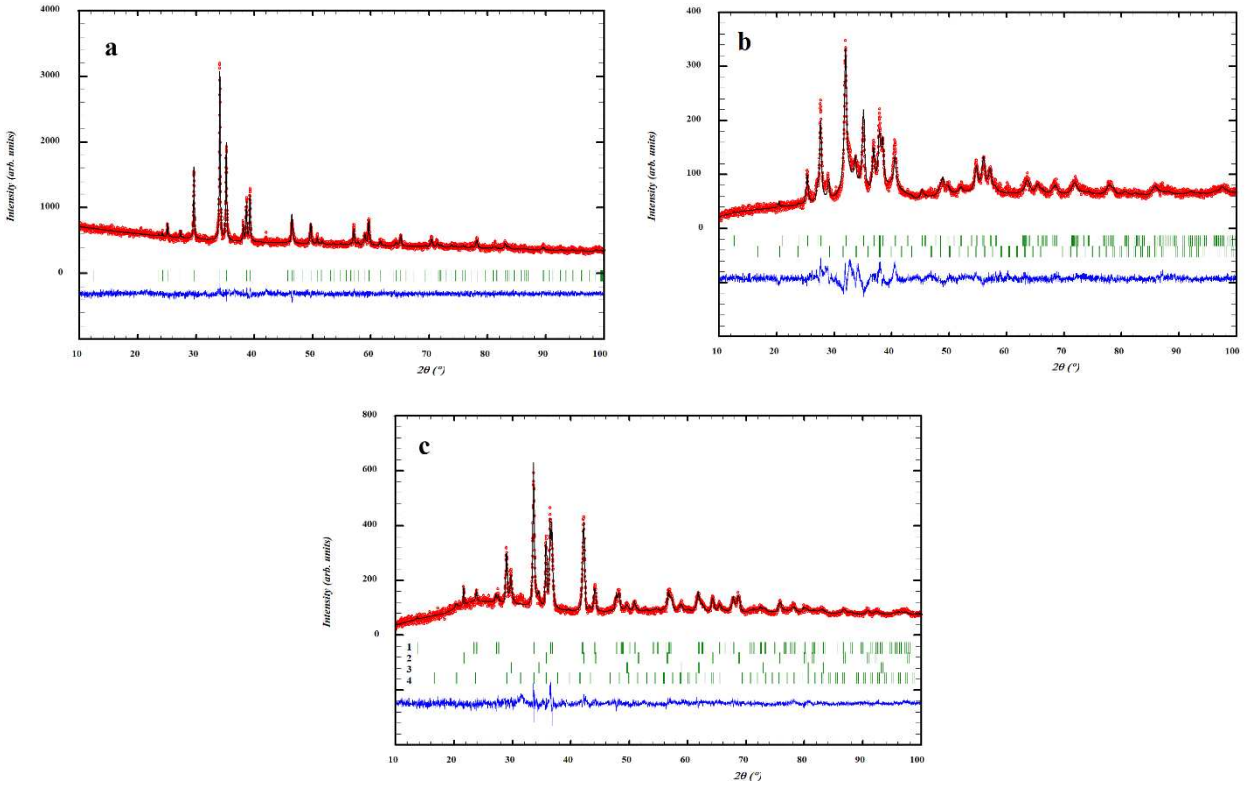

Fig. 2 X-ray powder patterns and positions of the Bragg reflections of the phases, for the samples Dy_2Ni_2In (Cu $K\alpha_1$ radiation) (a), and $Dy_2Ni_2InH_{4.5}$ (b), and the products of the thermal desorption of the hydride (Cu $K\alpha$ radiation): 1– DyNiIn, 2 – $DyNi_2$, 3 – DyH_2, 4 – Dy_2O_3) (c).

Table 1 Cell parameters *a*, *b*, *c*, *V*, their relative change upon hydrogenation $\Delta a/a$, $\Delta b/b$, $\Delta c/c$, $\Delta V/V$, atomic coordinates *x*, *y*, *z* of the metal atoms, Bragg and profile reliability factors R_B, R_p for Dy_2Ni_2In and its hydride.

Dy_2Ni_2In (space group *Cmmm*), R_B = 7.65 %, R_p = 3.91 % *a* = 3.904(1) Å, *b* = 14.145(3) Å, *c* = 3.664(1) Å, *V* = 202.35(9) Å^3				
Atom	Site	*x*	*y*	*z*
Dy	4*j*	0	0.3638(2)	½
Ni	4*i*	0	0.1953(5)	0
In	2*a*	0	0	0
$Dy_2Ni_2InH_{4.5}$ (space group *Cmmm*), R_B = 9.81 %, R_p = 5.36 % *a* = 4.440(1) Å, *b* = 14.045(4) Å, *c* = 3.722(1) Å, *V* = 232.1(1) Å^3 $\Delta a/a$ = 13.7 %, $\Delta b/b$ = -0.7 %, $\Delta c/c$ = 1.6 %, $\Delta V/V$ = 14.7 %				
Atom	Site	*x*	*y*	*z*
Dy	4*j*	0	0.3604(3)	½
Ni	4*i*	0	0.1841(7)	0
In	2*a*	0	0	0

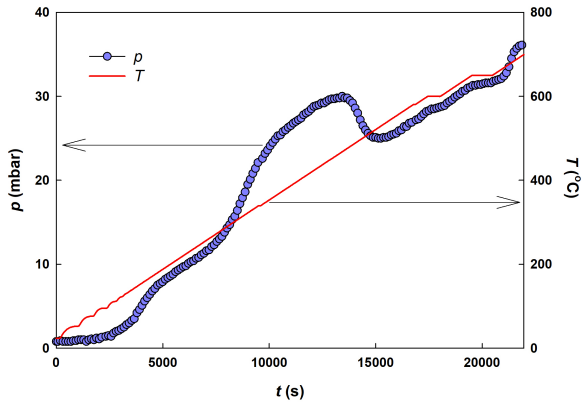

Fig. 3 Decomposition curve for the hydride $Dy_2Ni_2InH_{4.5}$, obtained in a closed system.

3.2 Hydrogenation of $Dy_2Ni_2In_{0.8}X_{0.2}$ (X = Al, Ga)

The partial replacement of In atoms in Dy_2Ni_2In by atoms of another *p*-element, here Al or Ga, led to the formation of a phase with the tetragonal structure type Mo_2FeB_2. However, annealing at 600°C removed the tetragonal phase while a phase with the orthorhombic Mn_2AlB_2 structure type was formed. Differential scanning calorimetry was used to determine the temperature of the phase transition. For the sample $Dy_2Ni_2In_{0.8}Al_{0.2}$, a sharp peak was observed at 892°C, both on the heating and cooling curve, which can indicate that the tetragonal phase forms above this temperature (Fig. 4). The transition takes place at a still higher temperature in the case of $Dy_2Ni_2In_{0.8}Ga_{0.2}$ (around 924°C). For this reason, as-cast samples were selected for the studies of the hydrogenation properties of tetragonal phases close in composition to Dy_2Ni_2In.

The solubility of Al in Dy_2Ni_2In was confirmed by electron microscopy and EDS analysis. The element mapping of the surface of the as-cast sample $Dy_2Ni_2Al_{0.2}In_{0.8}$ is shown in Fig. 5a. The main phase is In-rich, and the EDS analysis yielded the following composition: Dy – 37(2) at.%, Ni – 37.1(7) at.%, Al – 5.7(1) at.%, In – 20.2(1) at.%. The results exclude the formation of the previously reported off-stoichiometric phase with vacancies on the Ni site, and confirm the incorporation of Al. The Al:In ratio is close to the nominal composition. A spurious Al-rich phase with the following composition: Dy – 36(2) at.%, Ni – 45.1(9) at.%, Al – 14.5(3) at.%, In – 4.4(2) at.%, was observed. Besides, trace amounts of Dy_2O_3 were present in the sample, shown as red spots on the map.

The solubility of Ga in Dy_2Ni_2In was also confirmed by EDS analysis (Fig. 5b). The main phase is rich in In, and its composition is Dy – 38(2) at.%, Ni – 39.1(6) at.%, Ga – 1.9(1) at.%, In – 21.0(7) at.%. The composition of the spurious Ga-rich phase is Dy – 39(2) at.%, Ni – 44.6(7) at.%, Ga – 12.9(3) at.%, In – 3.5(1) at.%. The *M*:In ratio is somewhat lower than for the Al compound, meaning a lower Ga solubility limit in Dy_2Ni_2In.

The phase analysis of the as-cast samples $Dy_2Ni_2Al_{0.2}In_{0.8}$ and $Dy_2Ni_2Al_{0.2}Ga_{0.8}$ revealed minor amounts of the impurity phases $Dy_2Ni_2Al_{1-x}In_x$ and $Dy_2Ni_2Ga_{1-x}In_x$, respectively, with crystal structures of the W_2CoB_2 type (space group *Immm*).

Hydrogenation of the alloys $Dy_2Ni_2In_{0.8}Al_{0.2}$ and $Dy_2Ni_2In_{0.8}Ga_{0.2}$ was performed at room temperature under hydrogen pressures of 850 mbar and 870 mbar, respectively. In the case of $Dy_2Ni_2In_{0.8}Al_{0.2}$ hydrogenation started 300 s after introducing hydrogen into the system and reached saturation in 1800 s (Fig. 6). The amount of hydrogen absorbed corresponds to the formula $Dy_2Ni_2In_{0.8}Al_{0.2}H_{4.2}$. The hydrogenation process was more sluggish for $Dy_2Ni_2In_{0.8}Ga_{0.2}$. Hydrogen sorption started only after 45 minutes and lasted for another 30 minutes. The hydrogen content was 3.7 H at./f.u., which is lower, than for the Al compound.

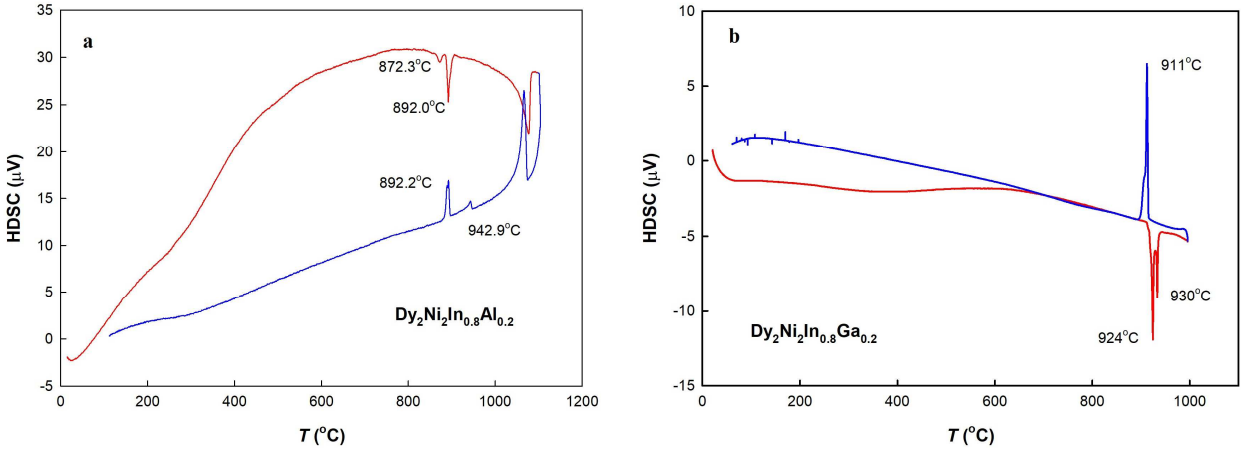

Fig. 4 DSC curves for $Dy_2Ni_2In_{0.8}Al_{0.2}$ (a) and $Dy_2Ni_2In_{0.8}Ga_{0.2}$ (b) samples (heating (red) and cooling (blue) rate 10 K/min).

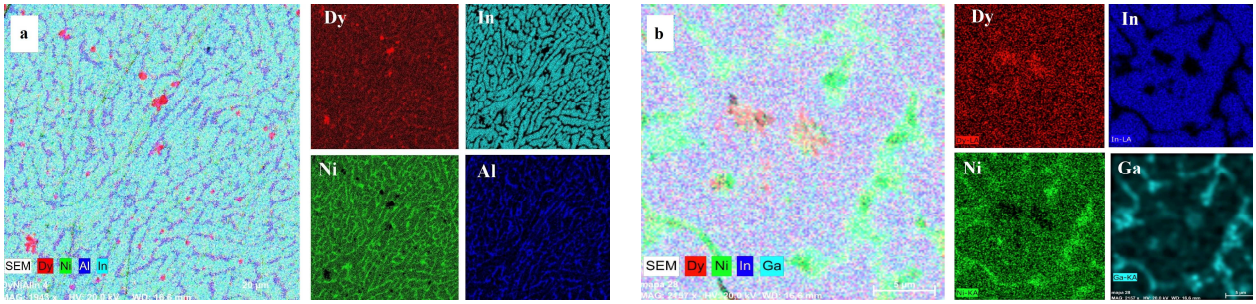

Fig. 5 Element mapping from EDS analysis of the as-cast alloys $Dy_2Ni_2In_{0.8}Al_{0.2}$ (a) and $Dy_2Ni_2In_{0.8}Ga_{0.2}$ (b).

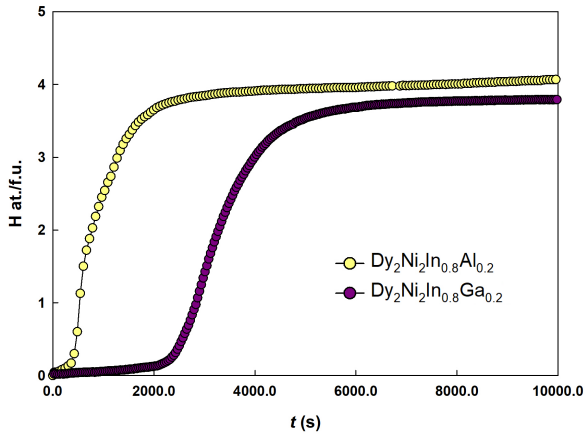

Fig. 6 Hydrogenation curves for $Dy_2Ni_2In_{0.8}Al_{0.2}$ ($p(H_2)$ = 850 mbar) and $Dy_2Ni_2In_{0.8}Ga_{0.2}$ ($p(H_2)$ = 870 mbar) at room temperature.

The effect of hydrogenation on the crystal structure of $Dy_2Ni_2In_{0.8}Al_{0.2}$ and $Dy_2Ni_2In_{0.8}Ga_{0.2}$ was studied by X-ray powder diffraction. The results of the structure refinement are given in Table 2, and the X-ray powder patterns of $Dy_2Ni_2In_{0.8}Al_{0.2}$ and $Dy_2Ni_2In_{0.8}Al_{0.2}H_{4.2}$ are shown on Fig. 7. The structure of the metal atom matrix was not changed upon hydrogenation. The relative volume expansion exceeds 9 % in both cases, and the lattice expansion is more pronounced in the *ab* plane. The peaks on the X-ray pattern are not substantially broadened after hydrogenation, meaning that, unlike Dy_2Ni_2In, there is no indication for a systematic decrease of the grain size.

4. Discussion

Dy_2Ni_2In, with orthorhombic Mn_2AlB_2-type structure, opens a new group of compounds that can form hydrides. The compound absorbs hydrogen from the gas phase under relatively mild conditions: room temperature and a hydrogen pressure below ambient. However, the process rate is relatively slow (several hours) and does not surpass that of related tetragonal compounds. A special feature of these compounds is strong uniaxial lattice deformation upon hydrogenation.

Doping Dy_2Ni_2In with atoms of other *p*-elements (Al or Ga) reveals new possibilities to stabilize the tetragonal phase at elevated temperatures. Taking into account the equal number of valence electrons for the elements belonging to the 13 group, we assume the size factor predetermines the evolution of the Mo_2FeB_2 structure type. Al appears to be a more efficient choice, compared to Ga, as seen from the lower transition temperature and more extended homogeneity region. The nature of the doping *p*-element affects the hydrogenation behaviour of the intermetallic as well. Here again, Al demonstrated better performance than Ga: higher hydrogenation rate, and higher hydrogen content in the hydride. This observation goes in line with the extremely active behaviour of the compounds R_2T_2Al upon hydrogenation (orthorhombic W_2CoB_2 structure type), which absorb up to 6 H at./f.u. within several seconds at room temperature under hydrogen pressures below 100 mbar [11]. Their hydrogenation activity substantially surpasses that of the isotypic Ga- or Sn-containing compounds.

A comparison of the effect of hydrogenation on the crystal structures of the Mn_2AlB_2- and Mo_2FeB_2-type compounds shows that hydrogenation has similar impact on the height of the constituent AlB_2- and CsCl-type slabs ($\Delta c/c$ = 1.6 % for the Mn_2AlB_2 type and $\Delta c/c$ = 1.3-1.9 % for the Mo_2FeB_2 type structures), but the arrangement of the fragments (columns) in the tetragonal structure type maintains the structure tighter, than the parallel slabs in the orthorhombic structure. In both cases hydrogenation hardly affects the distance from the *p*-element atom in the CsCl-type structure fragment to the nearest Ni atom (the distance even decreases for orthorhombic Dy_2Ni_2In). Instead, the distance that is significantly affected upon hydrogenation is the Ni–Ni distance between atoms inside the trigonal prisms forming the AlB_2-type slabs. Hence, one can presume similar positions for the hydrogen atoms in the two structures and the defining role of the AlB_2-type fragments in the formation of hydrides.

Table 2 Cell parameters *a*, *c*, *V*, their relative change upon hydrogenation $\Delta a/a$, $\Delta c/c$, $\Delta V/V$, atomic coordinates *x*, *y*, *z* of the metal atoms, Bragg and profile reliability factors R_B, R_p for $Dy_2Ni_2In_{0.8}Al_{0.2}$, $Dy_2Ni_2In_{0.8}Ga_{0.2}$, and their hydrides.

$Dy_2Ni_2In_{0.8}Al_{0.2}$ (space group *P*4/*mbm*), R_B = 5.88 %, R_p = 2.59 % *a* = 7.3586(8) Å, *c* = 3.6561(4) Å, *V* = 197.97(4) Å^3				
Atom	Site	*x*	*y*	*z*
Dy	4*h*	0.1751(2)	0.6751(2)	½
Ni	4*g*	0.3783(5)	0.8783(5)	0
($In_{0.8}Al_{0.2}$)	2*a*	0	0	0
$Dy_2Ni_2In_{0.8}Al_{0.2}H_{4.2}$ (space group *P*4/*mbm*), R_B = 9.99 %, R_p = 3.58 % *a* = 7.639(3) Å, *c* = 3.705(2) Å, *V* = 216.2(2) Å^3 $\Delta a/a$ = 3.8 %, $\Delta c/c$ = 1.3 %, $\Delta V/V$ = 9.2 %				
Atom	Site	*x*	*y*	*z*
Dy	4*h*	0.1752(4)	0.6752(4)	½
Ni	4*g*	0.3764(9)	0.8764(9)	0
($In_{0.8}Al_{0.2}$)	2*a*	0	0	0
$Dy_2Ni_2In_{0.8}Ga_{0.2}$ (space group *P*4/*mbm*), R_B = 4.55 %, R_p = 5.20 % *a* = 7.3570(6) Å, *c* = 3.6598(4) Å, *V* = 198.08(3) Å^3				
Atom	Site	*x*	*y*	*z*
Dy	4*h*	0.1754(4)	0.6754(4)	½
Ni	4*g*	0.3766(9)	0.8766(9)	0
($In_{0.8}Ga_{0.2}$)	2*a*	0	0	0
$Dy_2Ni_2In_{0.8}Ga_{0.2}H_{3.7}$ (space group *P*4/*mbm*), R_B = 7.55 %, R_p = 6.40 % *a* = 7.627(1) Å, *c* = 3.7293(6) Å, *V* = 216.95(5) Å^3 $\Delta a/a$ = 3.7 %, $\Delta c/c$ = 1.9 %, $\Delta V/V$ = 9.5 %				
Atom	Site	*x*	*y*	*z*
Dy	4*h*	0.1705(3)	0.6705(3)	½
Ni	4*g*	0.3718(9)	0.8718(9)	0
($In_{0.8}Ga_{0.2}$)	2*a*	0	0	0

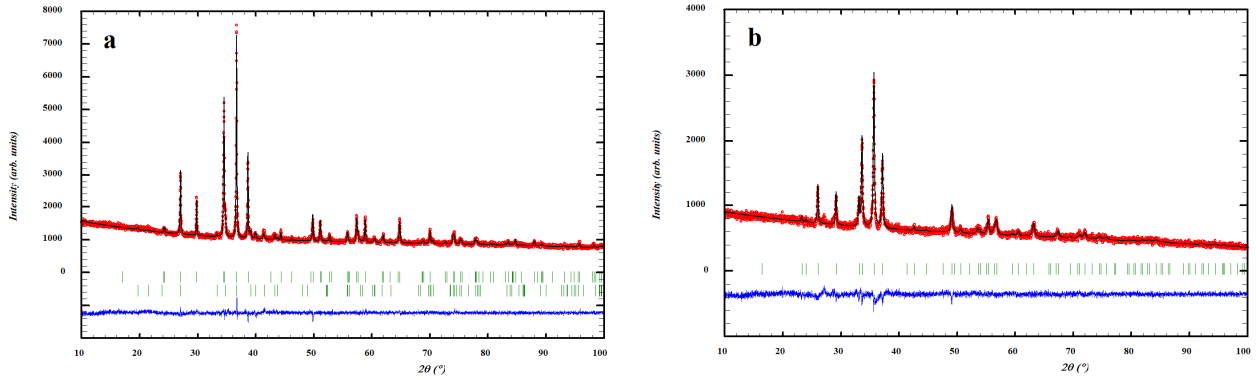

Fig. 7 X-ray powder patterns for the samples $Dy_2Ni_2In_{0.8}Al_{0.2}$ (a) and $Dy_2Ni_2In_{0.8}Al_{0.2}H_{4.2}$ (b) (Cu $K\alpha_1$ radiation).

Conclusions

The orthorhombic compound Dy_2Ni_2In opens a new group of intermetallics that can form hydrides at room temperature under hydrogen pressures below ambient, absorbing up to 4.5 H at./f.u. Hydrogenation results in strongly anisotropic (uniaxial) lattice expansion, while the relative volume expansion reaches 14.7 %.

A tetragonal phase based on the Dy_2Ni_2In compound can be obtained by substituting small amounts of Al or Ga for In. The compounds $Dy_2Ni_2In_{0.8}Al_{0.2}$ and $Dy_2Ni_2In_{0.8}Ga_{0.2}$ also absorb hydrogen at room temperature under hydrogen pressures of ~850 mbar, forming hydrides of composition $Dy_2Ni_2In_{0.8}Al_{0.2}H_{4.2}$ and $Dy_2Ni_2In_{0.8}Ga_{0.2}H_{3.7}$, respectively. Hydrogenation results in anisotropic lattice expansion prevailing in the *ab* plane.

Both structure types, Mn_2AlB_2 and Mo_2FeB_2, belong to a series of intergrowth structures containing

AlB_2- and CsCl-type structural fragments. We believe that the AlB_2-type related fragments primarily define the hydrogenation properties of intermetallics belonging to the structure series $R_{m+n}T_{2m}M_n$.

Acknowledgement

This work was supported by the Ministry of Education and Science of Ukraine under the grant No. 0121U109766. The Ukrainian-Czech cooperation work was supported by a project financed by the Ministry of Education and Science of Ukraine (Project No. 0122U002456) and by the Czech Ministry of Education, Youth and Sport. K.M. acknowledges the Simons Foundation (Award Number: 1037973) for its support.

References

[1] H.J. Becher, K. Krogmann, E. Peisker, *Z. Anorg. Allg. Chem.* 344 (1966) 140-147.
[2] E.I. Gladyshevskii, T.F. Fedorov, Y.B. Kuz'ma, R.V. Skolozdra, *Sov. Powder Metall. Met. Ceram*. 5 (1966) 305-309.
[3] V.I. Zaremba, V.A. Bruskov, P.Yu. Zavalij, Ya.M. Kalychak, *Neorg. Mater.* 24 (1988) 409-411.
[4] Ya.M. Kalychak, V.I. Zaremba, V.M. Baranyak, P.Yu. Zavalij,V.A. Bruskov. L.V. Sysa, O.V. Dmytrakh, *Neorg. Mater*. 26 (1990) 94-96.
[5] L. Havela, *J. Alloys Compd.* 895 (2022) 162721.
[6] L. Havela, S. Mašková, P. Svoboda, K. Miliyanchuk, A. Kolomiets, A. V. Andreev, *Chem. Met. Alloys* 6 (2013) 170-176.
[7] M. Dzevenko, K. Miliyanchuk, Ya. Filinchuk, O. Stelmakhovych, L. Akselrud, L. Havela, Ya. Kalychak, *J. Alloys Compd.* 477 (2009) 182-187.
[8] S. Mašková, L. Havela, S. Daniš, A. Llobet, H. Nakotte, K. Kothapalli, R. Černý, A. Kolomiets, *J. Alloys Compd.* 566 (2013) 22-30.
[9] J. Rodriguez-Carvajal, Recent developments of the program FULLPROF, *Commission on Powder Diffraction (IUCr), Newsletter* 26 (2001) 12-19.
[10] S. Suwarno, M.V. Lototskyy, V.A. Yartys, *J. Alloys Compd.* 8420 (2020) 155530.
[11] K. Miliyanchuk, L. Havela, Y. Tsaruk, S. Mašková, R. Gladyshevskii, *J. Alloys Compd.* 647 (2015) 911-916.